Fatigue Assessment for the Failed Bridge Deck Closure Pour at Mile Marker 43 on I-81

http://www.virginiadot.org/vtrc/main/online_reports/pdf/14-r12.pdf

ELIAS RIVERA
Graduate Research Engineer

EBRAHIM K. ABBAS
Graduate Research Engineer

WILLIAM J. WRIGHT, Ph.D., P.E.
Associate Professor

RICHARD E. WEYERS, Ph.D., P.E.
Professor

C.L. ROBERTS-WOLLMANN, Ph.D., P.E.
Professor

Via Department of Civil and Environmental Engineering
Virginia Polytechnic Institute and State University

Final Report VCTIR 14-R12

Standard Title Page - Report on Federally Funded Project

1. Report No.: FHWA/VCTIR 14-R12	2. Government Accession No.:	3. Recipient's Catalog No.:
4. Title and Subtitle: Fatigue Assessment for the Failed Bridge Deck Closure Pour at Mile Marker 43 on I-81		5. Report Date: April 2014
		6. Performing Organization Code:
7. Author(s): Elias Rivera, Ebrahim K. Abbas, William J. Wright, Ph.D., P.E., Richard E. Weyers, Ph.D., P.E., and C.L. Roberts-Wollmann, Ph.D., P.E.		8. Performing Organization Report No.: VCTIR 14-R12
9. Performing Organization and Address: Virginia Tech Transportation Institute 3500 Transportation Research Plaza Blacksburg, VA 24061-0105		10. Work Unit No. (TRAIS):
		11. Contract or Grant No.: 97825
12. Sponsoring Agencies' Name and Address: Virginia Department of Transportation 1401 E. Broad Street Richmond, VA 23219 Federal Highway Administration 400 North 8th Street, Room 750 Richmond, VA 23219-4825		13. Type of Report and Period Covered: Final Contract
		14. Sponsoring Agency Code:

15. Supplementary Notes:

16. Abstract:

Fatigue of reinforcing steel in concrete bridge decks has not been identified as a common failure mode. Generally, the stress range occurring in reinforcing steel is below the fatigue threshold and infinite fatigue life can be expected. Closure pour joints, however, may be vulnerable to fatigue if some specific design details are present. This research shows that fatigue was a likely contributor to the I-81 closure pour failure. It is much less likely that corrosion directly caused a strength failure but it is very likely that corrosion accelerated the onset of fatigue.

The joints in the I-81 deck had vertical joint faces that did not provide any means for shear transfer across the joint. The joints were located under a wheel load path and were located away from beams or other means of deck support. This created atypical conditions where shear forces across the joint due to wheel loads were carried only by the reinforcing steel. The stress range in the reinforcing steel is greatly magnified under this scenario thereby making fatigue a possibility.

New closure pour joints can easily be designed to prevent fatigue by providing structural support for both sides of the joint. Existing joints, however, need to be evaluated to determine if fatigue vulnerability exists. Lacking knowledge of the joint internal details, a simple differential deflection test can be performed to detect fatigue vulnerability. If the two sides of the joint are deflecting vertically relative to each other under wheel loads, than fatigue can be considered a possibility. No deflection indicates that fatigue is unlikely.

17 Key Words: Corrosion, reinforcement, decks, closure pours, fatigue, failure	18. Distribution Statement: No restrictions. This document is available to the public through NTIS, Springfield, VA 22161.		
19. Security Classif. (of this report): Unclassified	20. Security Classif. (of this page): Unclassified	21. No. of Pages: 40	22. Price:

Form DOT F 1700.7 (8-72)   Reproduction of completed page authorized

FINAL REPORT

**FATIGUE ASSESSMENT FOR THE FAILED BRIDGE DECK CLOSURE POUR
AT MILE MARKER 43 ON I-81**

Elias Rivera
Graduate Research Engineer

Ebrahim K. Abbas
Graduate Research Engineer

William J. Wright, Ph.D., P.E.
Associate Professor

Richard E. Weyers, Ph.D., P.E.
Professor

C.L. Roberts-Wollmann, Ph.D., P.E.
Professor

Via Department of Civil and Environmental Engineering
Virginia Polytechnic Institute and State University

DISCLAIMER

The project that is the subject of this report was done under contract for the Virginia Department of Transportation, Virginia Center for Transportation Innovation and Research.   The contents of this report reflect the views of the authors, who are responsible for the facts and the accuracy of the data presented herein. The contents do not necessarily reflect the official views or policies of the Virginia Department of Transportation, the Commonwealth Transportation Board, or the Federal Highway Administration. This report does not constitute a standard, specification, or regulation. Any inclusion of manufacturer names, trade names, or trademarks is for identification purposes only and is not to be considered an endorsement.

Each contract report is peer reviewed and accepted for publication by staff of the Virginia Center for Transportation Innovation and Research with expertise in related technical areas. Final editing and proofreading of the report are performed by the contractor.

ABSTRACT

Fatigue of reinforcing steel in concrete bridge decks has not been identified as a common failure mode. Generally, the stress range occurring in reinforcing steel is below the fatigue threshold and infinite fatigue life can be expected. Closure pour joints, however, may be vulnerable to fatigue if some specific design details are present. This research shows that fatigue was a likely contributor to the I-81 closure pour failure. It is much less likely that corrosion directly caused a strength failure but it is very likely that corrosion accelerated the onset of fatigue.

The joints in the I-81 deck had vertical joint faces that did not provide any means for shear transfer across the joint. The joints were located under a wheel load path and were located away from beams or other means of deck support. This created atypical conditions where shear forces across the joint due to wheel loads were carried only by the reinforcing steel. The stress range in the reinforcing steel is greatly magnified under this scenario thereby making fatigue a possibility.

New closure pour joints can easily be designed to prevent fatigue by providing structural support for both sides of the joint. Existing joints, however, need to be evaluated to determine if fatigue vulnerability exists. Lacking knowledge of the joint internal details, a simple differential deflection test can be performed to detect fatigue vulnerability. If the two sides of the joint are deflecting vertically relative to each other under wheel loads, than fatigue can be considered a possibility. No deflection indicates that fatigue is unlikely.

FINAL REPORT

FATIGUE ASSESSMENT FOR THE FAILED BRIDGE DECK CLOSURE POUR
AT MILE MARKER 43 ON I-81

Elias Rivera
Graduate Research Engineer

Ebrahim K. Abbas
Graduate Research Engineer

William J. Wright, Ph.D., P.E.
Associate Professor

Richard E. Weyers, Ph.D., P.E.
Professor

C.L. Roberts-Wollmann, Ph.D., P.E.
Professor

Via Department of Civil and Environmental Engineering
Virginia Polytechnic Institute and State University

INTRODUCTION

In 1992, several bridge decks on I-81 near Marion, Virginia, were replaced, using staged construction, as part of a bridge rehabilitation project (Sprinkel et al., 2010). Figure 1 presents a transverse section showing the width and location of the closure pour. Epoxy-coated reinforcement was used as the reinforcing steel. There was no formed keyway at the joint between the previously cast deck and the closure pour. After 17 years in service, a 3 ft by 3 ft closure pour section punched through, as shown in Figure 2. All of the bars along the closure/deck interface on both sides of the closure were severed.

The closure pour was positioned under the left wheel path of the southbound right lane of the bridge deck, so the joint was subject to a very large number of wheel loads. Observations at the bridge site indicated that the joint had opened slightly. In this case it is possible that the reinforcing bars alone were carrying shear and moment across the joint. The open joint also provides a more direct path for deicing salts to penetrate to the reinforcing bars and induce corrosion. Figure 3 shows a portion of the closure pour joint where the concrete was removed around the bars spanning across the joint. The brown coloration indicates degradation of the epoxy coating, there is evidence of corrosion in the bars, and the bars are fractured vertically close to the plane of the joint. There is little evidence of ductile deformation of the bars prior to fracture. This indicates that the bars failed in a brittle mode possibly due to fatigue and fracture. It is therefore likely that both fatigue and corrosion played a role in the failure of the closure.

TRANSVERSE SECTION
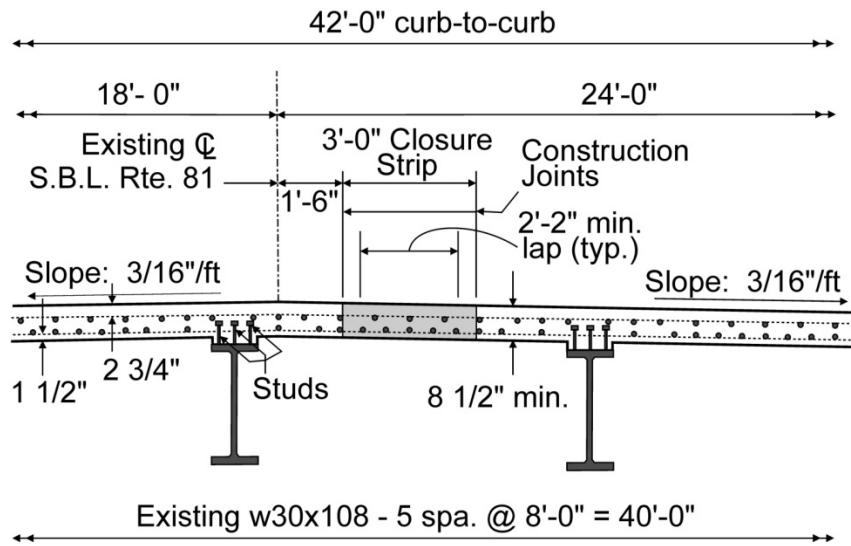
Figure 1. Transverse Section of Bridge Deck With Closure Pour

Figure 2. Failed Section of Closure Pour

Figure 3. Condition of Reinforcing Bars Spanning Across Joint Showing Corrosion and Vertical Break Through Bars

PURPOSE AND SCOPE

The purpose of this study was to investigate the influence of the fatigue and strength overload on the overall failure mechanism that occurred in the I-81 bridge deck slab. A separate report characterized the influence of corrosion on the failure process (Abbas et al., 2014).   This study focused on strength and fatigue testing of specimens to determine the mechanical effects on the failure process. Four 4.5 ft by 10 ft slab sections, containing the closure, were removed from the failed bridge deck to perform a series of tests. Specimens tested from these slabs have some pre-existing level of corrosion and fatigue damage from their service in the bridge. Three new slabs were fabricated in the lab, with the same design as the slabs removed from the actual bridge deck. These specimens were used to assess shrinkage and the cause of the joint opening observed in the field. In addition, these specimens served as undamaged controls for the fatigue and strength tests since there was no pre-existing damage.

Two types of testing were performed in this study. Strength tests were performed to evaluate the slab strength across the closure pour joint. The failure mode was studied to help determine if overloads contributed to the failure mechanism. A second series of tests subjected the slab specimens to cyclic loading to determine if fatigue contributed to the failure.

METHODS

Specimens

The study was conducted on a total of eleven specimens, eight from the actual I-81 failed bridge and three new specimens fabricated and cast in the lab.

I-81 Deck Slabs

Sections measuring approximately 4.5 ft by 10 ft were saw cut, removed from the bridge deck, and delivered to the Thomas Murray Structures Laboratory at Virginia Tech. The sections contained the entire closure pour section along with approximately 9 in of the adjacent deck slab, as shown in Figure 4. After examining the sections, eight test specimens, 22 in wide, were cut from the four slabs to be used for fatigue and strength testing. The 22-in specimens each contained two truss bars, one top straight bar, and one bottom straight reinforcing bar. A detailed characterization of the condition of the slabs and the specimen cut locations is provided in a separate report (Abbas et al., 2014).
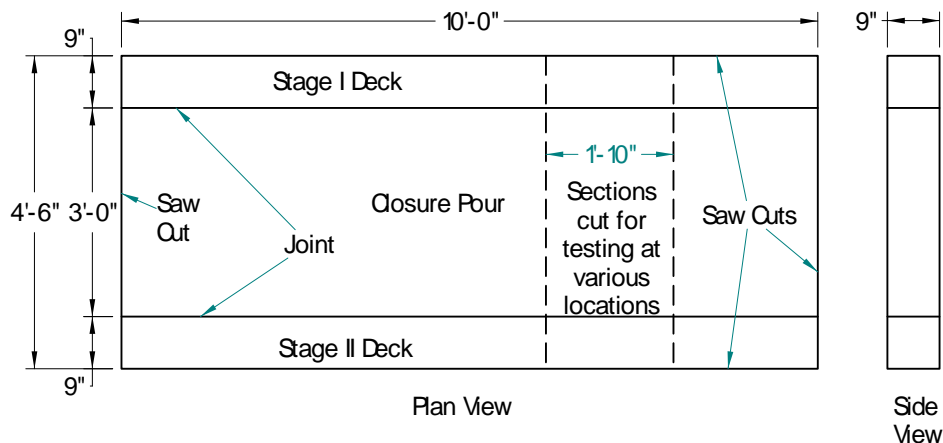

Figure 4. Approximate Dimensions of Slab Sections Showing Cuts Made to Extract Typical Test Specimen

Lab Cast Specimens

Three slab specimens were fabricated and cast in the lab. The concrete used in casting the slabs was A-4 ready mixed concrete, which is standard for Virginia bridge decks (4,000 psi at 28 days, Virginia Department of Transportation [VDOT] standard identification). The slabs were constructed to mimic the actual configuration of the slab, including the support beams. The actual deck and the lab specimen dimensions and reinforcing are presented in Figure 5.

The specimens were cast in two stages with the center section (closure pour) cast 30 days after the two end sections. The end sections were bolted to support beams to simulate the constraint of the two sides of the bridge. This resulted in some opening of the joints due to shrinkage of the closure pour concrete. Details of the casting sequence are provided in a separate report (Abbas et al., 2014).
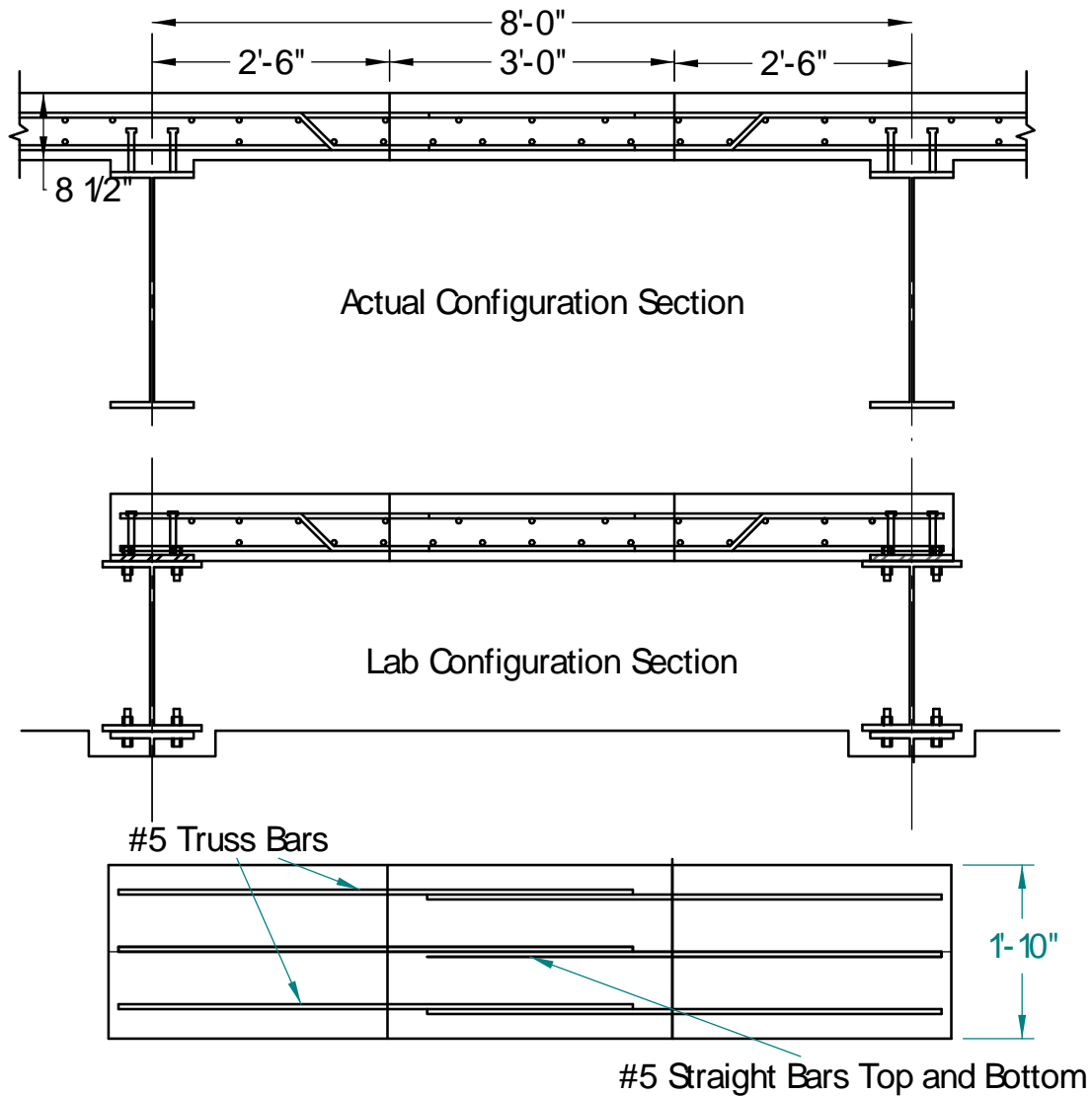
Figure 5. Lab Cast Slab Specimens Showing Reinforcing Steel Layout

Material Properties

The material properties of the I-81 and the lab cast slab specimens were measured prior to testing (Abbas et al., 2014). Core samples were taken and tested from the I-81 slabs that were in service for 17 years. Test cylinders were prepared during casting of the lab cast specimens. Table 1 shows the average values from multiple tests.

Table 1. Average Concrete Strength Properties in Test Specimens

Specimen Type	Location	Compressive Strength, ksi	Elastic Modulus, ksi	Tensile Strength, ksi
I-81 Slabs	Center	7.65	4,420	0.655
	End Blocks	5.66	3,760	0.563
Lab Cast Slabs	Center	6.40	6,110	0.650
(90-day strength)	End Blocks	6.65	4,580	0.760

The reinforcing steel for the lab cast slabs was No. 5 Grade 60 bars with a measured yield strength of 67.5 ksi. All bars were epoxy coated to match the actual bridge conditions. The properties of the reinforcing steel for the I-81 specimens were not measured but it was assumed to be typical strength for No. 5 Grade 60 bars.

Strength and Fatigue Testing

Basic Test Set-up

A three-point loading configuration was used for all tests to approximate the moment and shear occurring across the closure pour in the actual bridge. In the bridge, the slab is attached to multiple girders and some degree of two-way action can be expected. Since the failure occurred along the closure pour joint line it is reasonable to assume that one-way action dominated the failure. The test specimens, shown in Figure 6, are strips cut from the slab and are tested under one-way action. The point load shown in the figure was actually applied over a 10 in by 20 in elastomeric pad to simulate a truck wheel load in the actual bridge.
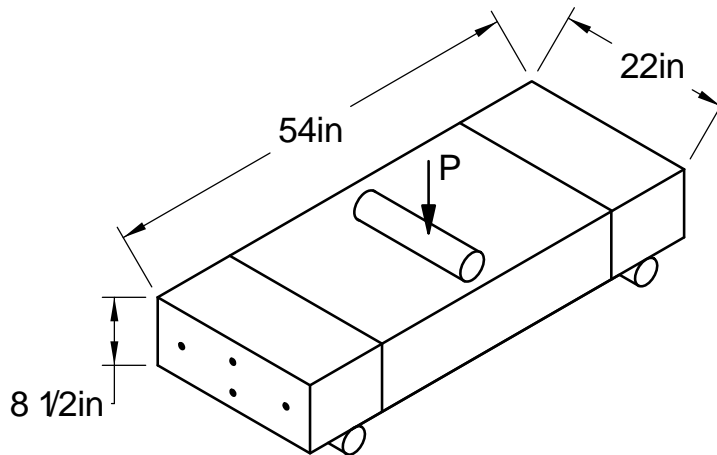
Figure 6. Testing Configuration of 22-in Slab Specimens

Figure 7 shows the approximate moment and shear diagrams that would be expected from a point load at the center of the closure pour in the I-81 bridge. The roller supports for the test specimens are located at inflection points in the moment diagram; therefore the moment diagram for the single span specimens approximates the moment diagram for the continuous slab. This results in moment and shear forces across the joint in the test specimens that are similar to what is expected in the actual bridge. However, this set-up does not consider any axial

6

tension force on the specimens due to constraint and shrinkage in the bridge. The presence of the joint is a local stiffness discontinuity in the deck. In the actual bridge, localized rotation at the joint is restricted due to the multi-span continuity of the slab. In the test specimens, higher local rotation occurs at the joint allowing the gap to close at the top of the joint. This allowed contact between the concrete on both sides of the joint and increased the local shear stiffness of the joint. The significance of this difference is discussed later in the report. However, given the limited length (9 in) available outside the closure pour, there was no feasible way to add constraint and axial force to the I-81 slab specimens.
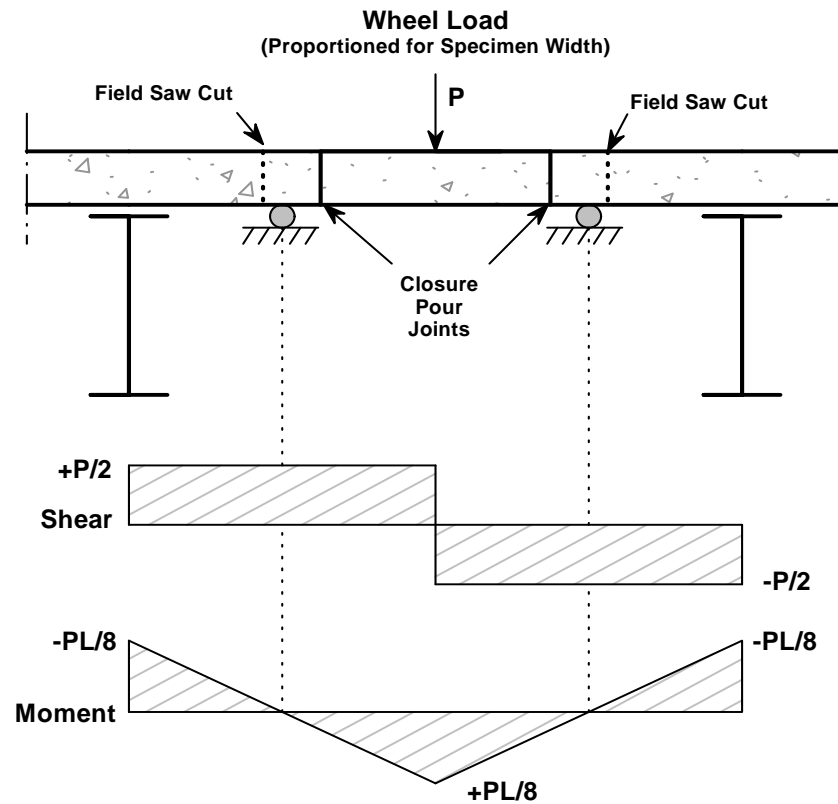
Figure 7. Comparison of Moment and Shear Diagrams for Continuous Slab in Bridge and Test Specimens

Figure 8 shows a schematic of the test set-up for both the fatigue and strength tests. Bearing plates were bolted on the top and the bottom of the end blocks to distribute the roller point load into the concrete. Because of the short length of the end blocks in the I-81 slab specimens, there was some concern that cracking and loss of development of the reinforcing steel could occur and jeopardize the test. The bearing plates helped provide confinement to the concrete. In addition, the bar ends were drilled and tapped to allow installation of end caps to improve the development strength of the bars. These measures were successful; no bar slip was observed during testing.

7
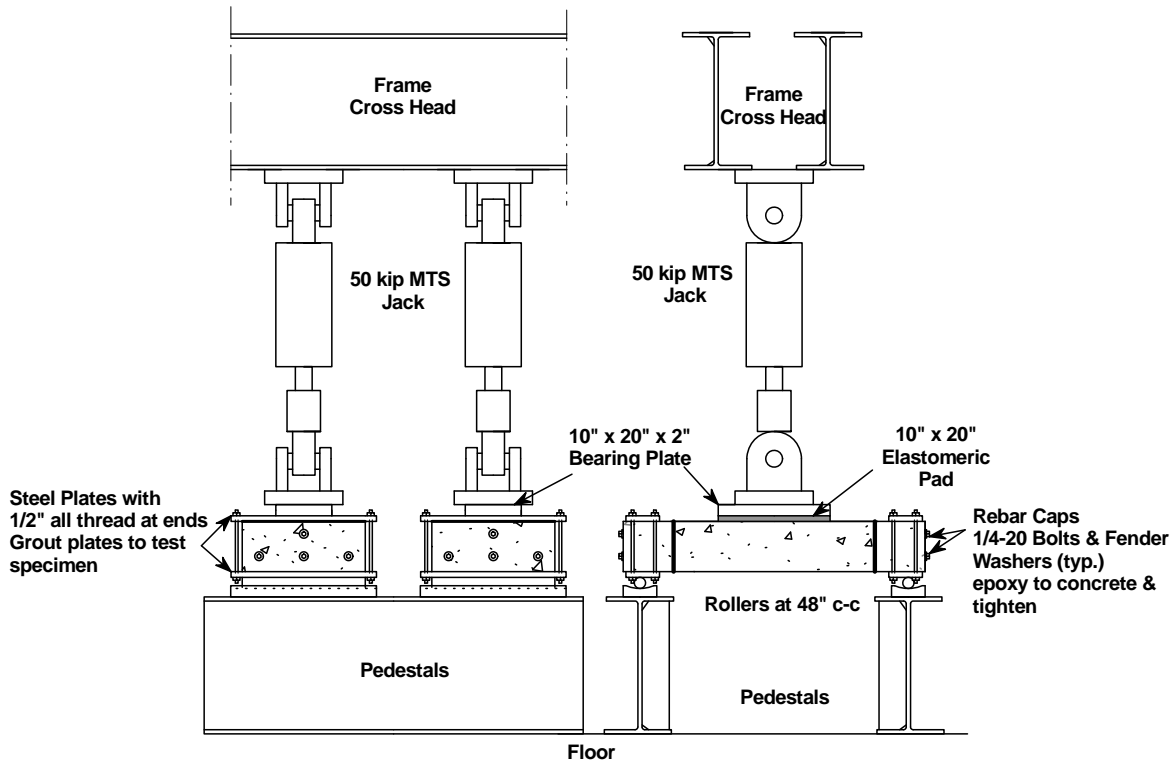
Figure 8. Schematic Showing Test Set-up for Strength and Fatigue Tests

Figure 9 shows the test set-up for the fatigue tests. Two independent specimens were tested in parallel to accumulate cycles on two specimens simultaneously. The same test set-up was initially used for the strength tests. However, somewhat unexpectedly, the 50-kip MTS jacks provided insufficient force to fail the specimens. The modified set-up, shown in Figure 10, replaced the MTS jack with a 100-kip static jack. The load patch and roller boundary conditions remained identical for the two set-ups.

As shown in Figure 5, the lab cast specimens had longer end blocks to simulate the actual 8 ft girder spacing present in the bridge. One of the three lab cast specimens was strength tested with the identical set-up shown in Figure 10. The support rollers remained at the 4 ft spacing and the longer end blocks cantilevered out on both ends. With some minor adjustment for self weight, both the I-81 and one of the lab cast slabs were all tested using the same set-up.

8

**Figure 9. Testing Set-up Using 50-kip Servo-hydraulic Jacks for Fatigue Tests**

Figure 10. Modification of Test Set-up to Enable Higher Loads to Achieve Failure in Strength Tests

9

Modified Axial Force Set-up

A modification was made to the basic testing set-up to introduce axial force to the specimen during testing. This configuration was used for one strength and one fatigue test. This modification allowed the joint to be jacked open during testing thereby minimizing the localized joint rotation effects previously discussed. Because of the limitations on end block length, it was possible to test the lab cast specimens using only this configuration.

The axial force was achieved by installing jacking struts on the two sides of the specimens. This is essentially a reverse post-tensioning system that adds tension instead of the usual compression to the specimen. Jack placement on the sides prevented interference with the load actuators, instrumentation, and roller supports. The jacking struts consisted of square HSS tubes with a manual screw jack welded to one end. Prior to application of the wheel load, the screw jacks were adjusted to provide the desired level of axial force across the joint.
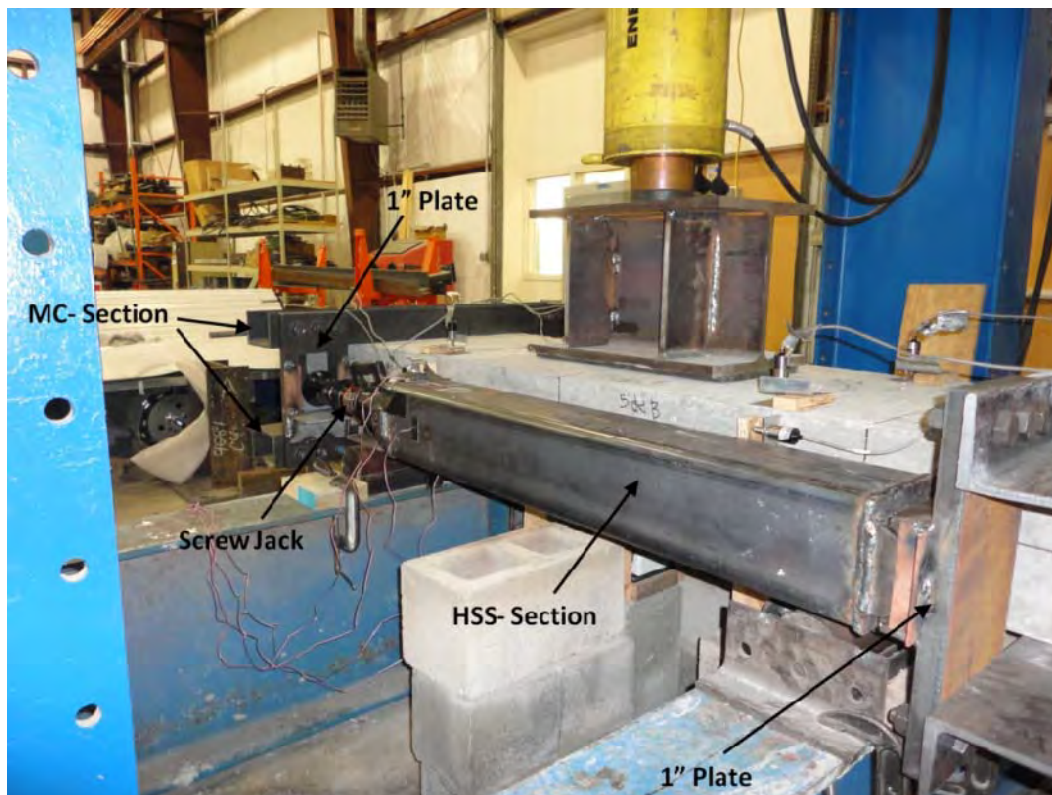
Figure 11. Jacking Struts Installed on Sides of Specimens to Add Axial Force Across Joints

The jacking struts bear on end plate assemblies that were bolted to the concrete end blocks with concrete anchor bolts. The end plate assemblies consist of MC6x18 channels that extend past the width of the specimen as shown in Figure 12. A 1-in steel bearing plate transfers the jacking force to the channels. The screw jack has a swivel head in contact with the bearing plate and a rocker was placed on the end of the HSS tube. This allowed the anchor blocks to rotate relative to the jacking strut. Therefore, the jacking struts had minimal effect on restraining rotation of the end blocks during testing.
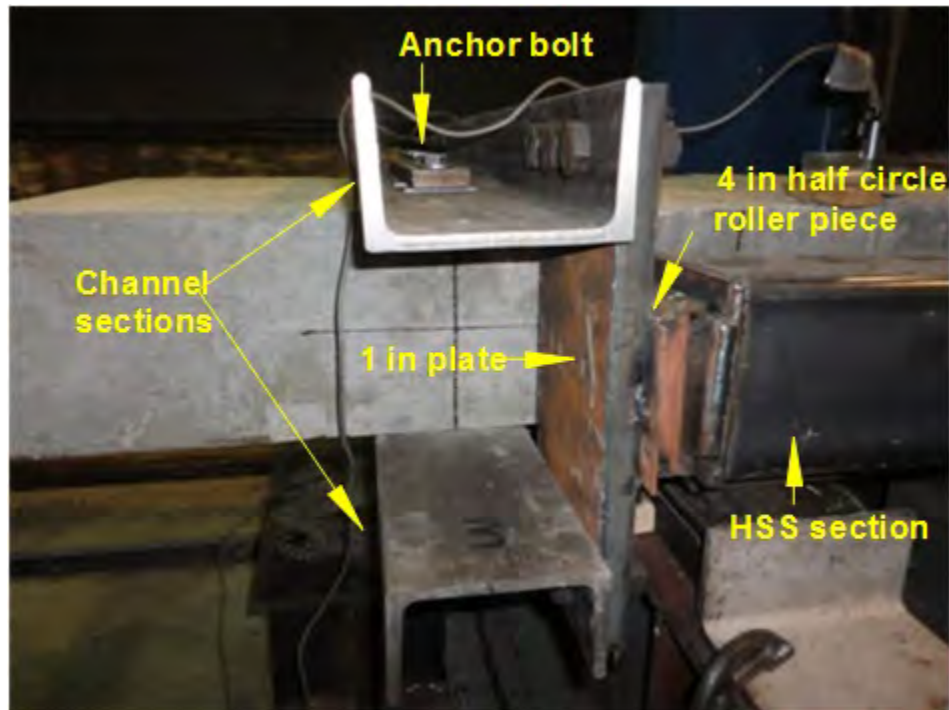
Figure 12. End Bearing Block to Transfer Jacking Strut Force to Concrete End Block

The jacking strut was placed with its centerline axis at the mid-depth of the slab specimens. This position provides no eccentricity to the concrete cross section. However, the presence of truss bars in the specimen resulted in an eccentricity of the reinforcing steel across the joints. The jacking therefore caused some rotation across the joints in addition to opening of the crack. Additional eccentricity was introduced when the specimens deflected vertically during testing. Both of these effects were considered when forces in the bars were analyzed.

Instrumentation

An array of instrumentation was installed and monitored with a computer-controlled data acquisition system. Load cells were used to measure the wheel load force for both the fatigue and strength tests. The vertical deflection of the slab specimens was measured using wire potentiometers. For some of the earlier I-81 tests, LVDTs were installed on the end blocks to monitor for any bond slip in the reinforcing steel during testing. This practice was discontinued after no slip was observed.

The horizontal opening and relative vertical displacement of the joints were measured during various stages of testing. LVDTs were mounted on the slab surface to measure the relative vertical deformation (shear deformation) occurring across the joint. Two LVDTs were installed on each joint to measure any differences across the width. Mechanical DEMEC gages were used to measure the horizontal opening of the joints at the top and bottom on each side of the specimen. The DEMEC readings were recorded manually at various stages while the loading

11

was held constant. Figure 13 shows that the DEMEC points were replaced with LVDTs for the lab cast slabs with the jacking struts to record joint opening better during the tests.
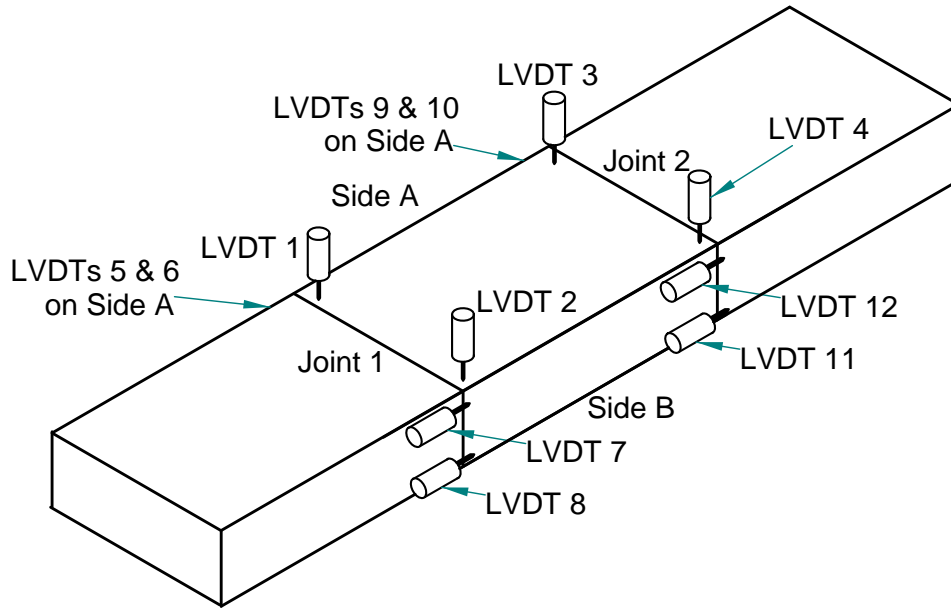
Figure 13. Additional LVDTs Installed on Sides of Specimen B to Monitor Opening of Construction Joints

Test Procedures

A total of nine tests were conducted for this research investigation as shown in Table 2. The I-81 specimens were all tested using the basic set-up. After the six tests were analyzed, it became apparent that the basic set-up was allowing the joint to close under the test loads. The modified axial force set-up was designed and implemented for two of the lab cast slabs. One of the lab cast slabs was tested using the basic set-up to help identify the set-up effect and the difference between the I-81 and lab cast specimens.

Table 2. Test Matrix Showing Test Type and Set-up for the Nine Test Specimens

Test Type	Basic Set-up		Modified Axial Force Set-up	
	I-81	**Lab Cast**	**I-81**	**Lab Cast**
Strength Test	Specimen 1			
	Specimen 3	Specimen C		Specimen B
	Specimen 8			
Fatigue Test	Specimen 2			
	Specimen 4			Specimen A
	Specimen 7			

Strength Test Procedure

The same procedure was followed for the strength tests of all the specimens except for Specimen B where the joints were opened with the jacking system prior to testing. The bearing

12

plates were aligned and grouted to the specimens to provide even bearing along the roller supports. The specimens were adjusted to place the 20 in by 10 in elastomeric pad in the center of the specimen with the load jacks plumb. The data acquisition system was programmed to record data 10 times per second and was operated continuously during the test. The loads were increased gradually and held constant at select levels to allow reading of the manual DEMEC gages. Failure was defined when the load began to decrease under increasing displacement. The rate of loading was controlled to provide a relatively constant displacement rate during the test.

Fatigue Test Procedure

The same specimen installation procedure was used for the fatigue tests and the strength tests. The fatigue tests were conducted by applying cyclic loads at a frequency of 3 Hz. The cyclic loading was continued until fatigue failure was observed or 10 million load cycles were applied to the specimens. A minimum load level of $P_{min} = 0.5$ kip was applied to ensure the jacks stayed in compression contact with the specimen through the entire load cycle.

Little is known about what load range would cause failure of the specimens within the 10 million cycle window. The 10 million cycle limit was chosen to allow completion of the tests within the duration of the project. It does not necessarily relate to the number of wheel load cycles that occurred in the bridge. The load range was initially set at 8 kips ($P_{max} = 8.5$ kips, $P_{min} = 0.5$ kip) to provide a reasonable wheel load to the specimen. The localized failure observed in the I-81 slab is governed by the number of wheel loads occurring directly on the joint. Heavier truck wheel loads will cause more fatigue damage compared to lighter loads. The AASHTO HS-20 truck specifies two 32-kip and one 8-kip axle load per truck. In reality, the 32-kip load is on a tandem axle; therefore an HS-20 truck will produce four 8-kip and one 4-kip wheel loads per truck passage over the joint.

The scaling effect must be considered between the 22-in-wide strip specimens and the actual bridge. When analyzing slabs by the strip method, an HS-20 truck wheel is assumed to act on a 72-in width of slab. A 16-kip wheel load acting on a 72-in strip equates to a 4.89-kip wheel load acting on a 22-in strip. The other unknown is the appropriate impact factor for the wheel load. AASHTO requires a 75% impact factor for fatigue of joints and a 15% impact factor otherwise. The reality for the closure pour joint probably lies somewhere between the two bounds. Based on this discussion, an initial load range of 8 kips was chosen for the first fatigue test. This was later increased to 16 kips after no failure was observed at 8 kips. It is recognized that 16 kips is an artificially high wheel load but 10 million cycles is an artificially low number for 17 years of truck traffic on I-81.

The fatigue tests were paused at logarithmic intervals (10^0, 10^3, 10^4, 10^5, 10^6, and 10^7) in the cycle count to measure the stiffness and behavior of the specimen. A slow speed test was performed from between $P = 0$ to P_{max} while recording all channels of instrumentation. The instrumentation cannot be read and recorded real-time during the fatigue cycling. The purpose of this procedure was to capture any time-dependent degradation of the specimen due to the fatigue loading.

13

Axial Force Jacking Procedure

For the two specimens that used the modified axial force set-up a compression force was placed in the jacking struts prior to any testing. The jack screws were gradually turned while recording data from the instrumentation. The jacking force was measured by monitoring strain gages on the HSS tubes.

A decision was made to perform the modified axial force tests with joints that were clearly open and across which there was no concrete-to-concrete contact in the joint. This represented conditions where all of the force across the joint was being carried by the rebar. The target jacking force level was therefore set to 20 kips per strut or 40 kips total across the joint. This force level was achieved in Specimen B but only 18 kips per jack was achieved in Specimen A. The jacking force was not adjusted during testing and there was a modest force loss over the duration of the tests. However, the joints remained fully open for the duration of testing.

RESULTS AND DISCUSSION

Strength Tests

There were a total of five strength tests conducted in this study. Three tests were on slab specimens cut from the I-81 bridge deck (Specimens 1, 3, and 8). The remaining two were on the cast specimens, one with the basic set-up (Specimen C) and the other with the jacking set-up (Specimen B). The load-displacement curves for all strength tests are shown in Figure 14. The shape of the load-displacement curve is similar for all tests. All specimens were loaded until a clear failure occurred defined as the point where the load began to decrease with increasing displacement. Specimen 3 was the only exception where the test was stopped at 88.3 kips before failure occurred. Specimen 3 was later retested, but the maximum load reached was only 74 kips. This suggests that the specimen was close to failure in the initial test at 88.3 kips.

The three I-81 specimens (1, 3, and 8) all showed similar load versus displacement behavior. The shape of the curves can be described as bi-linear with a "kink" occurring between 55 and 61 kips. The initial portions of the curves have similar slopes indicating similar elastic stiffness early in the test. The slopes are again similar in the portion of the curve immediately after the kink. Greater divergence develops later in the test as the ultimate load is approached and there is significant cracking in the concrete.

14
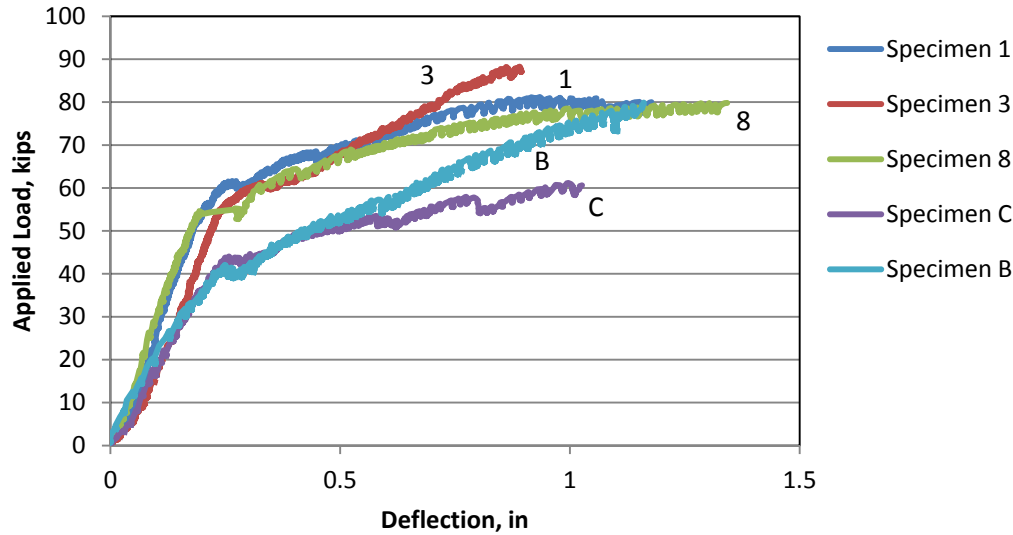
Figure 14. Load Versus Vertical Deflection for the Five Strength Tests

The two newly cast specimens (B and C) showed similar behavior that again can be described as bi-linear. Compared to the I-81 specimens, the two newly cast specimens exhibited lower stiffness in the initial elastic portion of the curve. The kink occurs at approximately the same displacement as the I-81 specimens but at a much lower load level. The initial post-kink portions of all five curves appear to have similar slopes although the load level is lower for the lab cast specimens. Again, the curves diverge at higher load levels, approaching the ultimate load, when significant cracking is present in the specimens.

Table 3 shows the maximum load and mid-span deflection measured during the test. Also shown are the maximum calculated moments based on two assumptions for distribution of the wheel load and the maximum shear during the test. The jack load was applied on a 10 in x 20 in elastomeric pad. As the specimen deflects, this results in a non-uniform pressure distribution on the specimen with higher contact pressure at the edges of the loading pad. Therefore the maximum moment at mid-span is not exactly known and the two loading assumptions shown in Figure 15 bound the value. The distributed load moment in Table 3, based on a uniform contact pressure assumption, provides an upper bound on the actual mid-span moment. The two-point load assumes that the non-uniform contact pressure can be approximated by two point loads 16 in apart. This forms a lower bound on the actual moment. The actual mid-span moment lies somewhere between these two bounds.

Table 3. Summary of Strength Test Results

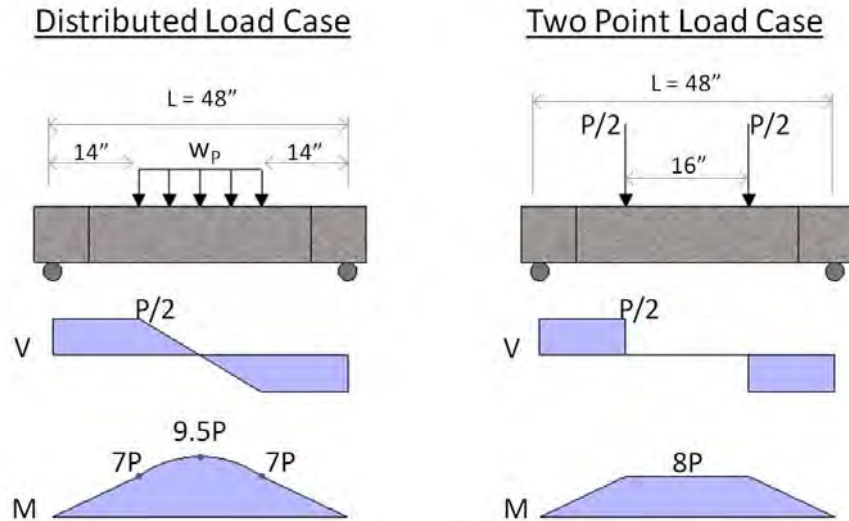| Specimen Identification	Ultimate Load (kip)	Midspan Deflection (in)	Distributed Load Moment (in-kip)	Two Point Load Moment (in-kip)	Ultimate Shear (kip)
Specimen 1	81.2	0.926	771	650	40.6
Specimen 3	88.3	0.891	839	706	44.1
Specimen 8	79.8	1.340	758	638	39.9
Specimen C	61.2	0.996	581	490	30.6
Specimen B	79.9	1.161	759	639	39.9

15

Figure 15. Two Extreme Loading Situations Resulting From Applied Wheel Load

Analysis of I-81 Specimen Strength

The load-displacement curves for the I-81 specimens along with the calculated shear and flexural limits are shown in Figure 16. The flexural limits for the two loading assumptions were calculated based on the Whitney stress block method using the average concrete strength of 7.65 ksi. The shear limit was determined based on shear strength of the concrete slab. The kink in the load-displacement curve occurred between the bounds of the two flexural strength predictions and slightly above the shear strength prediction. However, the ultimate strength of the specimens significantly exceeded the strength predictions. Because the specimens are much shorter than typical concrete beams, it is likely that the beam strength prediction models do not accurately predict strength for the specimens. The effects of the load patch and construction joints can also introduce error into the strength predictions.

The slab specimens behaved like homogeneous beams despite the presence of the two construction joints. The typical cracking pattern shown in Figure 17 shows that the two joints are outside of the failure zone and do not significantly participate in the failure. There was no measurable differential shear displacement across the joint until severe cracking occurred in the latter stages of testing. The cracking pattern appears to be primarily shear cracking with some contribution of flexure. This looks somewhat like a one-dimensional punching shear failure of the one-way slab. There are no shear cracks closer to the roller supports even though the end block concrete has lower strength and the shear load is the same as at the crack locations. This can therefore be classified as a local "punching type" failure under the wheel load that was influenced by bending of the specimen.

16
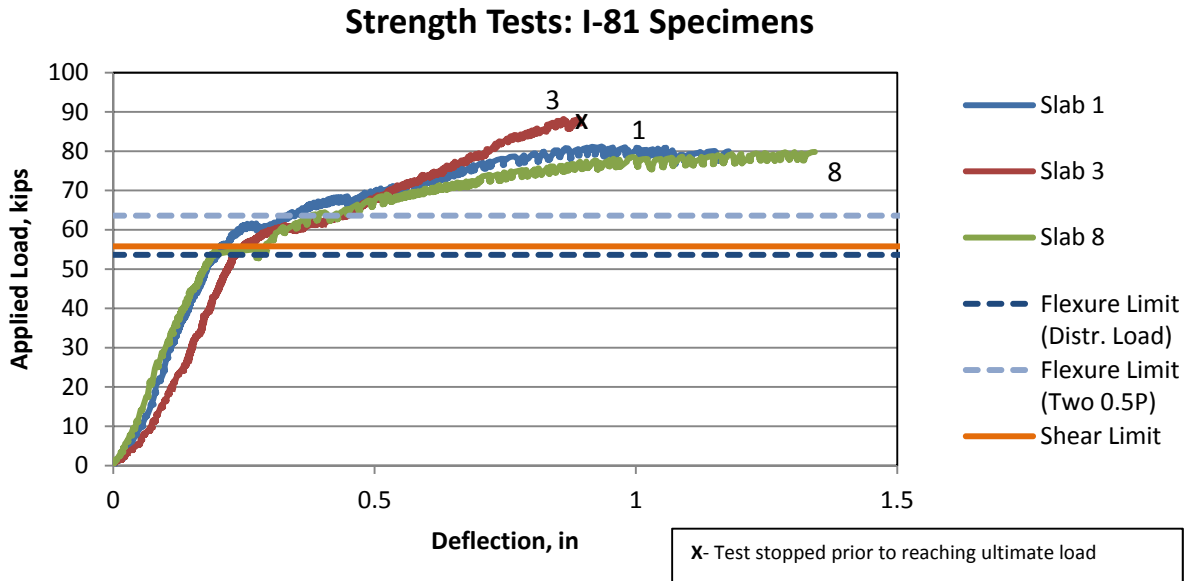
Figure 16. I-81 Load-Displacement Curves Compared to Calculated Flexural and Shear Limits

Figure 17. Typical Failed I-81 Specimen with Concrete Cracking Pattern Marked In Red

Analysis of Lab Cast Specimens

The load-displacement curves of the lab cast specimens are shown in Figure 18 along with the flexural and shear capacity predictions. The capacity predictions are based on an average strength of 6.33 ksi for the two specimens. Unlike the I-81 specimens, the kink occurs below the predicted strength. The elastic portion of the curves and the region immediately after

17

the kink are very similar between the two tests. However, once they reach the predicted shear limit the curves diverge. Specimen C, tested under the basic set-up without the jacking struts, failed close to the flexural capacity prediction for the two-point load assumption. The curve for Specimen B, tested with the jacking set-up that opened the construction joints, reached significantly higher capacity compared to Specimen C.
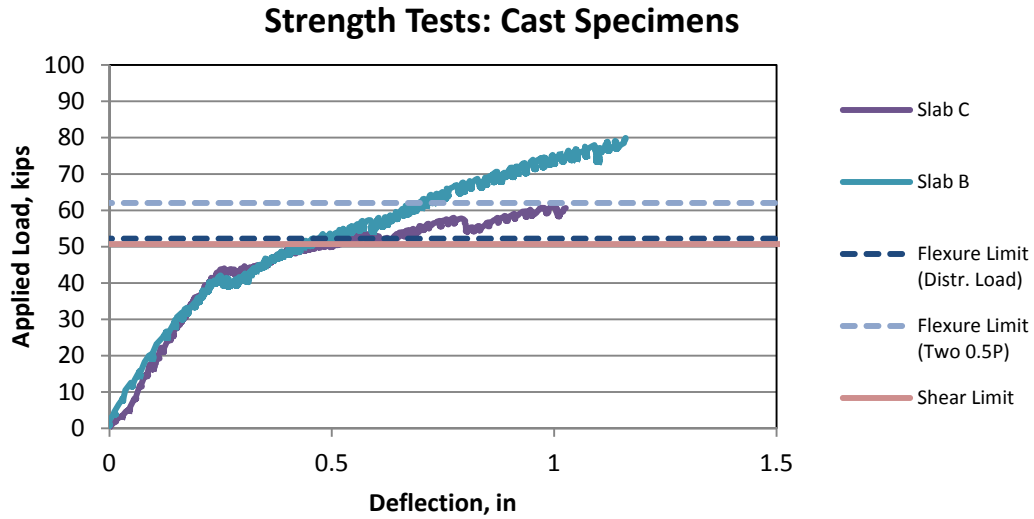
Figure 18. Load-displacement Curves for Lab Cast Specimens Showing Predicted Flexural and Shear Strength

Specimen C did not have any significant differential shear deflection across the construction joints during the early stages of testing below 42 kips. Beyond that load, there was some surface spalling of the "cream" layer on top of the slab at the LVDT locations that invalidated the readings. Figure 19 shows the post-failure cracking pattern for Specimen C. Overall, there were fewer cracks compared to the I-81 specimens and less crack branching. However, the two main cracks defining the failure mode are very similar to those in the I-81 specimens. This again appears to be primarily a punching-type failure that is influenced by flexural cracking. None of the cracking occurred in the end block or around the construction joints.   The failure was confined to the closure pour portion of the specimen.

Figure 19. Failure of Specimen C Showing the Two Main Cracks That Dominated the Failure Mode

Specimen B had the jacking struts installed and the specimen was pre-tensioned prior to testing. Figures 20 and 21 show the jacking force (in each strut) versus the joint opening displacement for each of the LVDTs that are shown in Figure 13. The actual crack opening in the I-81 bridge was not recorded prior to cutting the slab and the cutting process can be expected to relax constraint allowing the joint to close somewhat. Therefore, the joints were jacked to an arbitrary load level that clearly opened the joint.   The unsymmetrical pattern of the reinforcing steel creates an eccentricity across the joint where the jacking force is resisted by the reinforcing bars without any contribution from the concrete. This caused the crack to open more at the top compared to the bottom of the specimen during jacking. It appears that LVDTs 8 and 9 malfunctioned since no displacement was recorded during the test. The remaining LVDT readings show the top of the joints opening more than the bottom. The curves for all functioning LVDTs remained relatively linear indicating the reinforcing bars remained elastic during the jacking process. The jacking force was slowly increased until a load of 20 kips per strut (40 kips total axial load on the specimen). The jacking force slowly decreased during application of the wheel load during strength testing. The rate of decrease accelerated after the load exceeded about 45 kips and concrete cracking was observed.
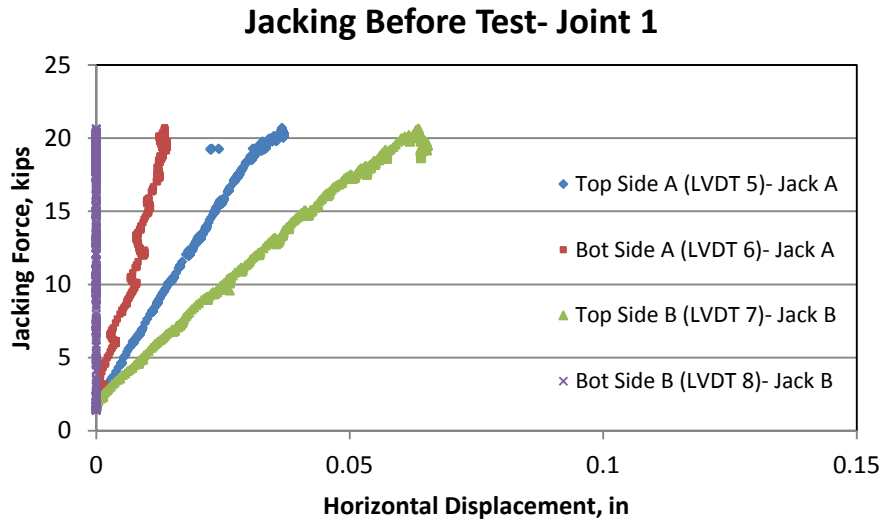
Jacking Before Test- Joint 1

Figure 20. Joint Opening LVDT Readings at Joint 1 During Jacking

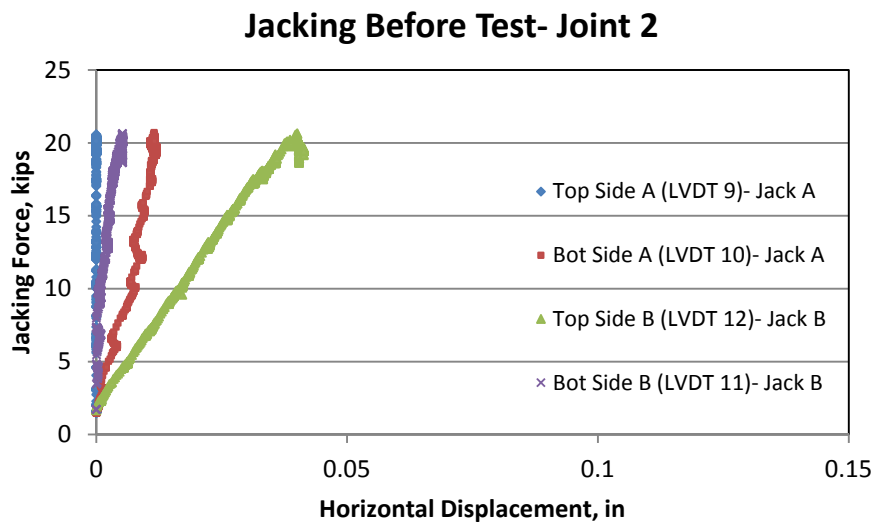## Jacking Before Test- Joint 2

Figure 21. Joint Opening LVDT Readings at Joint 2 During Jacking

Figure 22 shows the evolution of the deflected shape for Specimen B throughout the strength test. Because the deflection is measured at only five discrete points, the shape of the deflection curves is somewhat misleading. The rise at the two ends reflects uplift of the cantilevered sections of the end blocks. The center three points show a relatively constant deflection with the center point a bit larger in magnitude compared to the quarter points. However, there is a large increase between the deflection at the quarter points compared to the roller supports. This is shown as a straight line between the points; however most of this increase was due to localized shear deformation occurring at the construction joint. This contrasts with the non-jacking tests where the differential joint deflection was essentially zero.

20
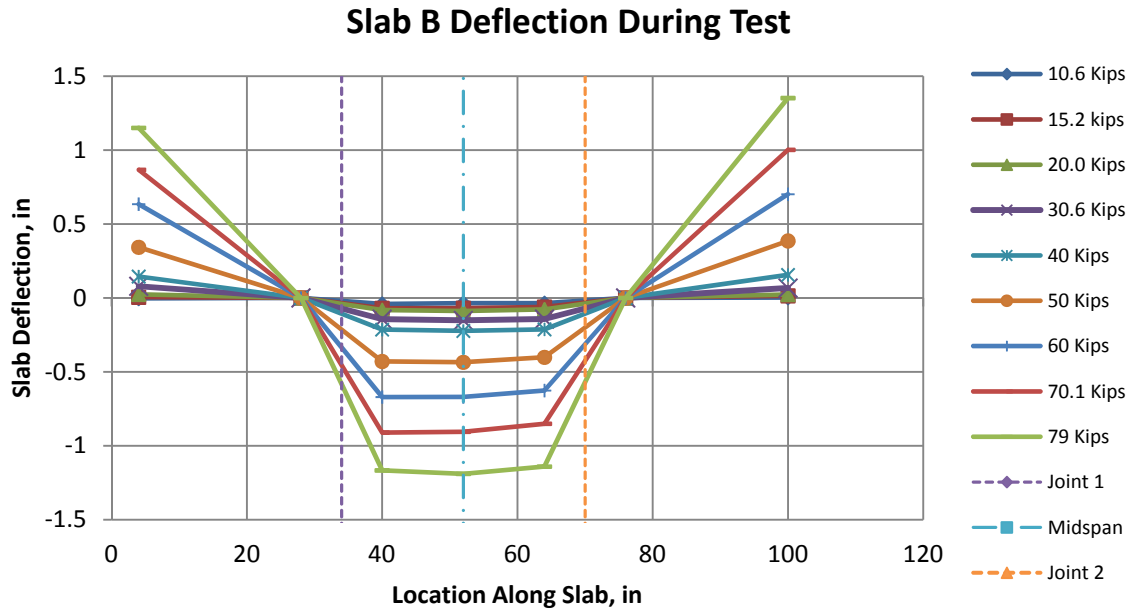
Figure 22. Deflected Shape of Specimen B at Various Load Levels Up to Failure

Figure 23 shows Specimen B after failure when the instrumentation and jacking struts were removed. The primary cracks defining the failure, marked in red, again show the punching-type shear failure similar to the previous tests. There is a clearly visible permanent vertical differential deflection across the two construction joints that is consistent with the shape shown in Figure 22.

Figure 23. Failure Mode in Specimen B That Was Tested With the Jacking Struts. The vertical differential deflection across the construction joints is readily apparent.

21

Discussion of Strength Tests

The one-way slab specimens used for the strength tests are a simplification compared to the two-way action that will occur in the I-81 bridge. However, the tests were effective in creating reasonable force conditions across the construction joint. However, the specimens without the jacking struts do not accurately recreate the continuity constraint present in the actual bridge. The lack of multi-span continuity allows a localized rotation to occur at the construction joints that effectively closes the joint at the top of the specimen. This enhances concrete-to-concrete contact across the joint. This concrete can therefore carry shear across the joint due to friction and interface contact. No differential vertical deflection was observed across the joints in any of the tests without the jacking struts. It can therefore be concluded that the forces in the reinforcing steel across the joint are similar to what would be expected if the joints did not exist, assuming a cracked concrete section in bending.

The ultimate failure mode in all of the strength tests was a punching-type failure underneath the load patch. This is not a pure punching shear failure that would be expected in a two-way slab but it has similarities to that mode in one dimension. In all cases, both jacked and un-jacked, the failure that limited ultimate capacity occurred in the closure pour section and did not involve the construction joints. The one specimen that was jacked experienced substantial differential vertical displacement across the joint but did not fail at that location. The failure still occurred in the closure pour section in the punching-type mode. This indicates that strength failure at the construction joints is not likely to occur under a wheel load when there is no corrosion damage to the reinforcing steel.

Figure 14 shows that the onset of cracking (the kink) occurs at lower load for the lab cast specimens compared to the I-81 specimens. This can be largely explained by the difference in strength between the specimens. The strength of the I-81 specimens is about 21 percent greater than the lab cast specimens in the closure pour region where the failure occurred. The difference in the kink location is approximately equal to the difference in strength. The strength effect is less clear at ultimate load where the scatter in the data increases.

No conclusions can be drawn about loss of strength in the I-81 slab specimens due to corrosion of the reinforcing steel. The I-81 specimens were limited by the short end blocks and the concrete clearly carried some of the shear and moment across the joints during testing. This probably masked any loss of strength that may be present across the joints due to section loss in the rebar. The local condition of the rebar across the joint is not known since the failure did not occur at the joints and the rebar was not visible after testing.

The consistency of the failure mode across the tests indicates that punching shear failure would have been the most-likely failure mode if a large wheel overload occurred in the I-81 bridge. However, the test strengths greatly exceeded the reasonable magnitude of a wheel load on the bridge. It is difficult to relate the test strength to an actual wheel load in the bridge since the 22-in slab specimens do not capture two-way action and actual wheel loads typically occur in tandem pairs. No evidence of punching-type failures were observed in the I-81 slab. The strength tests do not positively rule out strength failure in the I-81 bridge. However, it can be

concluded that strength failure of the reinforcing steel at the construction joints is highly unlikely unless there is extreme section loss of the reinforcing steel due to corrosion.

The strength tests show that openness of the construction joint has a significant effect on local differential deflections occurring across the joint. If the joint is held sufficiently open to prevent concrete contact, the reinforcing steel must carry all shear and moment across the joint. The tests showed that open joints experience clear differential vertical deflection between the two sides of the joint under the presence of a wheel load on the closure pore section. Joints that are not open do not experience this deflection. This suggests that field measurements of joint deflection under the presence of a wheel load may be a feasible method of assessing joint-openness for bridges in service.

Fatigue Tests

There were a total of four specimens tested under fatigue loading in this study. Three of these specimens were cut directly from the I-81 closure pour slabs and the remaining specimen was one of the lab cast specimens. The three I-81 specimens were tested with the basic test set-up, and the cast specimen was tested with the applied axial force from the jacking set-up. This section presents the results of fatigue tests and includes a discussion of the results.

Fatigue Test Procedure

Cyclic wheel loads were applied to the test specimens at a frequency of 3 Hz. The MTS test controller automatically monitors the load cell and maintains the desired load range (P_{max} and P_{min}) during testing. Therefore the specimens were tested under load control and any change in specimen stiffness did not affect the load levels. It was not possible to monitor the LVDTs and displacement transducers in real time during testing. The stiffness change in the specimen was monitored by pausing the cyclic loading at periodic intervals, installing the displacement transducers, and performing a static load test from zero to P_{max} while recording both load and displacements. The slope of the load versus mid-span displacement curve defines the basic specimen stiffness in kips per inch. The initial stiffness was measured before application of any cyclic loading. Additional stiffness measurements were performed after fatigue cycles were applied to detect any stiffness change due to cyclic loading. The stiffness measurements were performed at logarithmic cycle count intervals corresponding to 10^0, 10^3, 10^4, 10^5, 10^6, and 10^7 cycles.

The cyclic loading was continued until either fatigue failure occurred or 10 million cycles were applied to the specimen. The cycle limit was arbitrarily set as a practical limit on test duration within the period of performance of the testing program. The 10 million cycle limit has no direct relationship to the number of wheel load cycles seen by the specimens in service. The number of wheel loads over 17 years of service can be estimated as:

$$N = (365)(17)n(ADTT)_{SL} \qquad \text{(Eq. 1)}$$

Assuming the single lane average daily truck traffic $(ADTT)_{SL} = 4,000$ and three wheel load cycles per truck passage $(n = 3)$, it can be estimated that the closure pour experienced about 74 million cycles. Therefore, testing to a limit of 10 million cycles can be considered accelerated testing and a load range higher than the actual wheel load in the bridge will be required to obtain failure.

Stiffness Degradation During Testing

Figure 24 shows the stiffness variation of the four fatigue test specimens over the duration of cyclic testing. The stiffness of the five strength tests are plotted at 10^0 cycles for comparison. There is a large difference in the initial stiffness measured for the nine specimens. Some of this difference can be attributed to tolerance differences between specimens and differences in the roller support boundary conditions. However, the main cause of this difference is the non-linear nature of the load versus deflection data. The presence of the construction joints in the specimens is the main cause of non-linear response. Since the load level for fatigue cycling is well below the proportional limit observed in the strength tests, elastic material response is expected. However, this apparently does not apply to the joint interface. No clear pattern could be determined in the non-linear data that could be related to a physical event such as closure of the joint. Since the shape of the load versus displacement curve was significantly different for each stiffness measurement, there was significant variation in the correlation (R^2) of the individual stiffness measurements.

Because of the difficulty with using linear regression to calculate stiffness, it was not possible to observe any reliable stiffness change trends during the fatigue cycling. As shown in Figure 24, some specimens tended to show a slightly increasing stiffness and some a slightly decreasing stiffness over the duration of testing. It was originally hoped that stiffness could serve as an indicator of fatigue damage. However, this proved to be impractical for the test specimens used in this study.

24
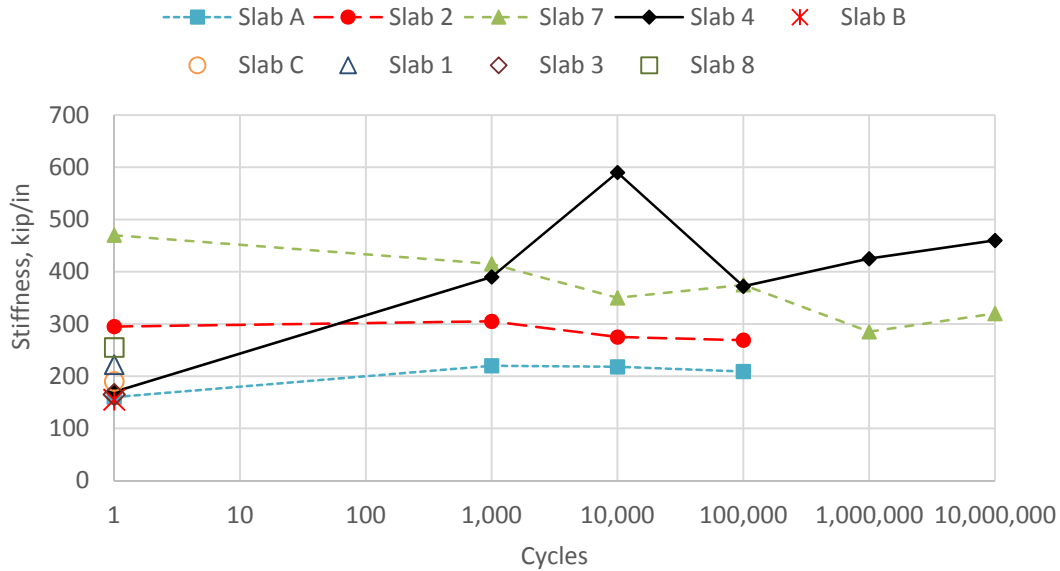
Figure 24. Specimen Stiffness Change in Fatigue Tests Over Duration of Testing. The stiffness of the static test specimens is shown at 10^0 cycles for comparison.

## I-81 Specimen Fatigue Results

Three specimens from the I-81 slabs (Specimens 2, 4, and 7) were fatigue tested to 10 million cycles without any evidence of fatigue failure. Specimen 4 was tested first at a load range of 8 kips (0.5 to 8.5 kips). This represented a relatively high wheel load compared to what would be expected for the joints in service. The decision was made to double the load range for Specimens 2 and 7 and they were tested with a 16-kip load range (0.5 to 16.5 kips). This represented an unrealistically high wheel load compared to service conditions. Again, no fatigue failure was observed after 10 million cycles.

There was no guidance in the literature concerning what fatigue life could be expected for the specimens with the joints. Prior testing performed by Helgason et al. (1976) was performed on bending specimens without joints. The fatigue failures in these tests occurred at points of maximum moment where the stress range in the reinforcing steel could be calculated based on a global flexural stress distribution model. The current tests have the added complication of the construction joints where the stress in the reinforcing steel is caused by a combination of global flexure, global shear, and local flexure and shear due to joint displacement.

Figure 25 shows the instrumentation locations for measuring displacements of the joints under the cyclic loading. The instruments were monitored only during the static stiffness measurements. Four LVDTs were used to measure the differential vertical displacement between the two sides of each joint. The measured differential vertical displacement was below the measurement resolution of the LVDTs (0.0001 in). This indicates that there was no differential vertical displacement between the two sides of the joint. Therefore, the local flexural and shear stresses in the reinforcing steel were essentially zero in these tests. The stress range in the reinforcing bars can therefore be determined based on the global moment and shear

25

distribution in the specimen due to the applied loads. This bar condition is similar to the bar condition of the tests by Helgason et al. (1976), where there was no construction joint present in their test specimens.

The longitudinal crack opening displacement across the joints was monitored using DEMEC gages that were mounted on the side faces of the specimens. The DEMEC measurements include both elastic deformation of the concrete and crack opening displacement of the joint within the gage length. Figures 26 and 27 show the DEMEC readings recorded at each stiffness measurement during the duration of fatigue cycling. Although there was some measurement variability, the results can be considered typical for both joints in all three I-81 specimens. The top reading (compression) and the bottom reading (tension) were connected by a straight line assuming that plane sections remain plane under the applied loading. The horizontal dashed line shows the neutral axis location of the unsymmetrical reinforcing steel assuming no concrete contact across the joint. The measured neutral axis location from the DEMEC readings tends to be higher than that predicted by the reinforcing steel alone. This indicates some degree of concrete contact across the joint.
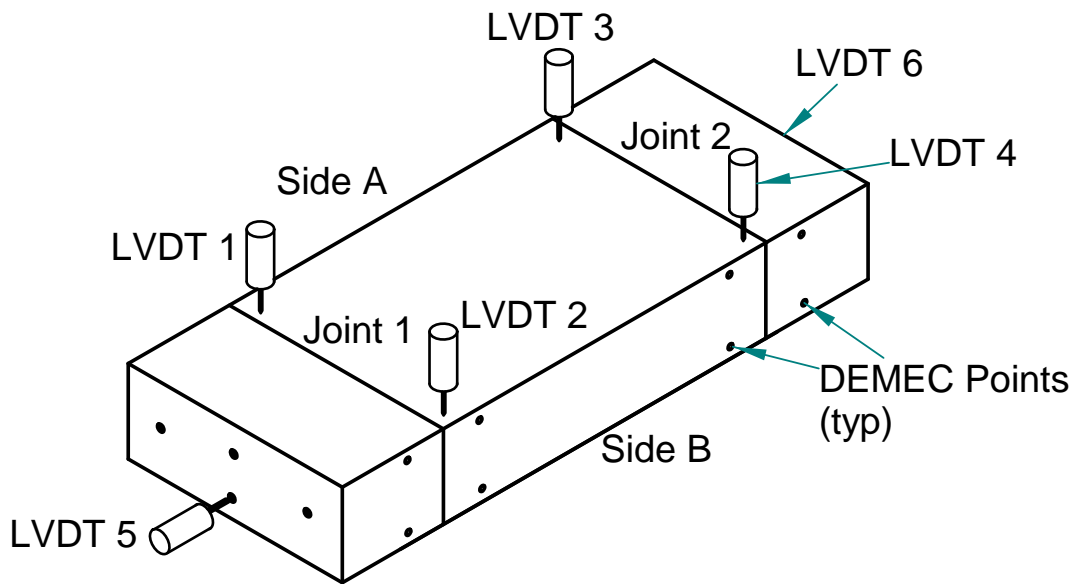
Figure 25. Instrumentation Locations for Measuring Joint Displacement in I-81 Fatigue Test Slabs
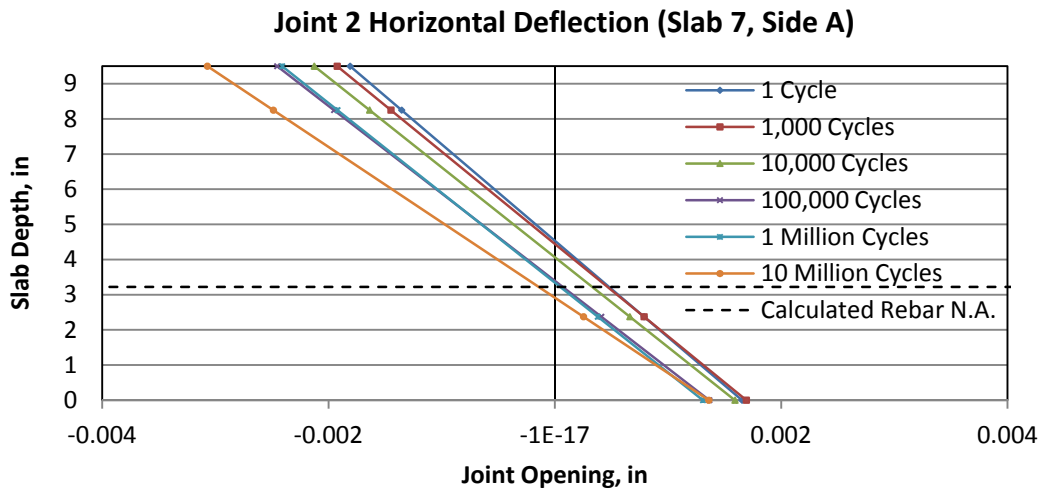
Joint 2 Horizontal Deflection (Slab 7, Side A)

Figure 26. DEMEC Measurements for Specimen 7 (Joint 2, Side A)

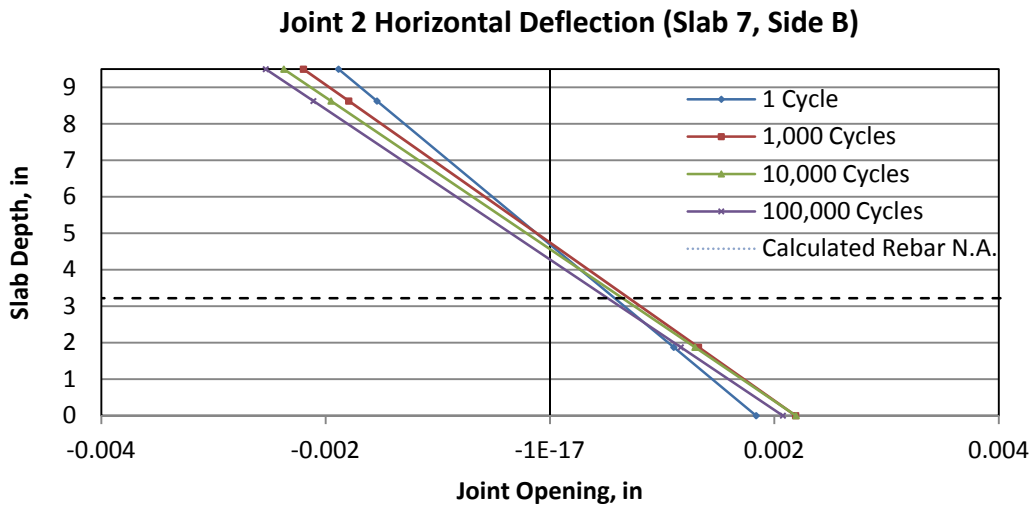**Joint 2 Horizontal Deflection (Slab 7, Side B)**

Figure 27. DEMEC Measurements for Specimen 7 (Joint 2, Side B)

The DEMEC readings on the compression side (top) of the specimens show a consistent change as cycles are accumulated on the specimens. This is shown by the increasing negative reading at higher cycle counts. The DEMEC gage provides a physical reference that is unaffected by zero balance or other electronic gage abnormalities. This trend shows that the degree of concrete contact is changing during the test. The joint tends to close more after fatigue cycles are accumulated on the specimen. The mechanism for this change is unknown but it may be attributed to wearing away debris and tighter contact of the concrete on opposite sides of the joint.

Interpretation of Results

No fatigue failures occurred in the I-81 slab specimens. However, analysis of the joint displacements occurring during the tests indicates this result is predictable. No differential

vertical displacement was measured across the joint under the fatigue load range. The DEMEC readings indicate that there is contact between the two concrete faces across the joint. This contact appears to be sufficient to carry shear across the joint through friction and interface contact of the concrete. This protects the reinforcing steel from local shear and bending deformation across the joint. The stress range in the reinforcing steel is therefore caused by the global bending and shear deformation of the specimen.   From a fatigue perspective, the specimens behaved as if there was no joint present. The global loading effects create a stress range in the reinforcing steel that is below the fatigue threshold established by Helgason et al. (1976).

The lack of joint displacement was not foreseen prior to testing of these specimens. The degree of joint openness is difficult to measure and presumably removing the slab sections from the bridge relaxed any shrinkage tension across the joint. The testing configuration provides a realistic approximation of the moment and shear occurring across the joint in the actual bridge. However, the roller supports do not provide the same rotational restraint that is present in the joint in the actual bridge. The roller supports allow the joint to rotate closed at the top in the test specimens while the two concrete faces will remain parallel in the actual bridge. Therefore, it can be concluded that the I-81 test specimens artificially increased concrete contact across the joint and protected the reinforcing steel from local joint deformation effects. In retrospect, these specimens were not useful for causing a fatigue failure in the reinforcing steel across the joint. However, they were useful in highlighting the significance of joint openness on the fatigue process.

## Lab Cast Specimen with Jacking System

The results of the I-81 specimen fatigue tests showed the importance of joint openness on the fatigue performance of reinforcing steel across the joints. The jacking system was devised to force the joint to remain open during fatigue testing and eliminate the beneficial effect of concrete contact across the joint. This should therefore represent a "worst-case" condition for fatigue of the reinforcing steel.

The test procedures and set-up for Specimen A were the same as for the I-81 specimens with the exception that the jacking system was added to open the joints. The instrumentation used to measure joint displacement was also changed as shown in Figure 28. LVDTs were used instead of DEMEC points to measure joint opening displacement.   Due to limited instrumentation availability, the joint opening displacement was measured for only one joint (Joint 1).
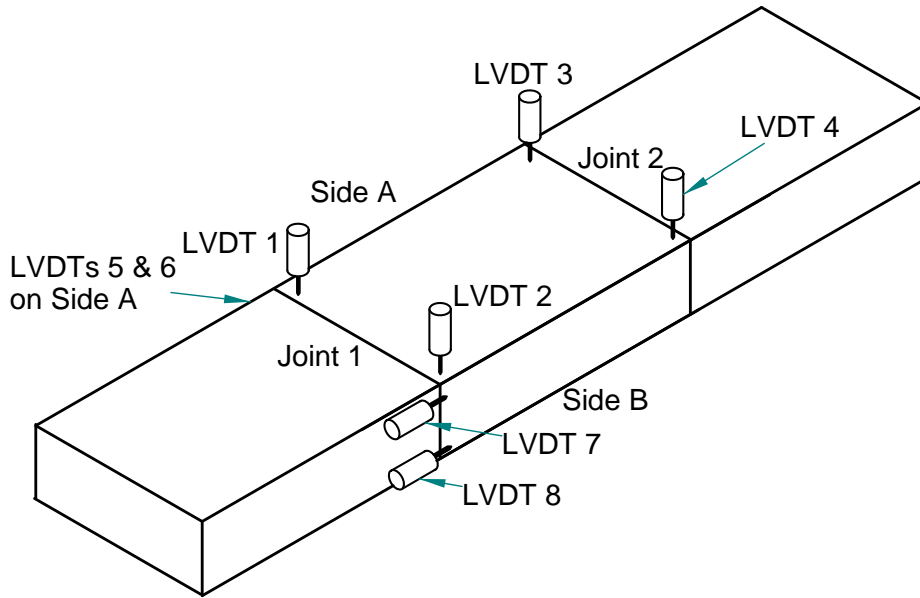
Figure 28. Lab Cast Specimen Showing LVDT Locations

Similar to the strength test with the jacking set-up (Specimen B), the joints were jacked open before testing using the jacking struts on both sides of the specimen. Since Specimen B was opened by applying a 20-kip load on each jacking strut, the same procedure was attempted for Specimen A. However, the jacking struts became difficult to turn and the jacking force was stopped at 18 kips. Since the joints were clearly opened at the 18-kip load, this was considered sufficient. Figure 29 shows that the jacking force decreased slightly over the duration of fatigue testing but remained essentially constant.
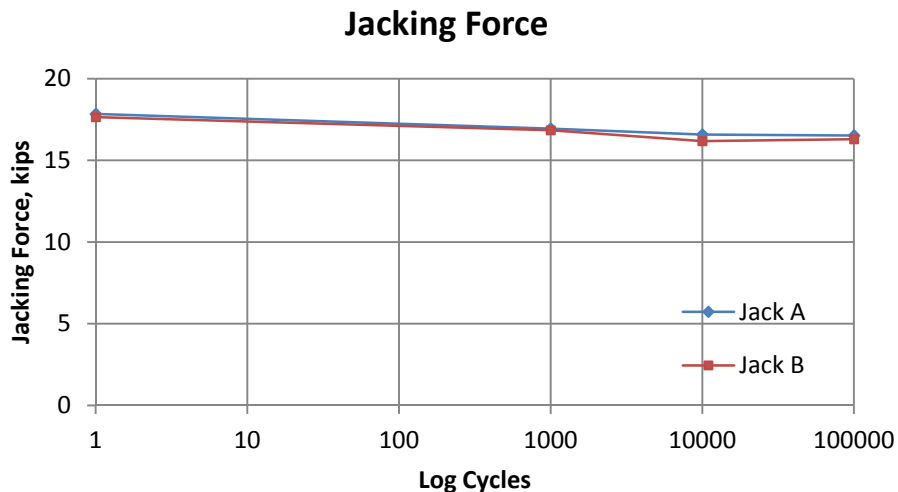
Figure 29. Jacking Force Over Duration of Fatigue Testing

The opening of the joints was monitored while the jacking force was applied to the specimen. Figure 30 shows the joint opening displacement for Joint 1. Although the jacking force for the fatigue specimen (Specimen A) was lower than the jacking force in the strength test (Specimen B), the top of the joint showed higher opening displacement. The joint opening displacements were essentially linear in Specimen B as shown in Figures 20 and 21. However, the joint opening displacement in Specimen A was non-linear and larger in magnitude as shown in Figure 30. The difference can be attributed to differences in eccentricity of the reinforcing steel group. The jacking struts were placed at the centerline of the concrete section. Because the reinforcing steel across the joint is not symmetric (one top, three bottom bars), this creates a force eccentricity in the reinforcing steel. Apparently the eccentricity was larger in Specimen B causing an increase in force in the top bar. Calculations indicate that the top bar probably exceeded yield in Specimen B thereby causing the non-linearity. It is difficult to calculate the strain in the yielded reinforcing bar precisely since the gage length inside the joint cannot be determined.

Yielding of the top reinforcing bar can be expected to have a relatively minor effect of fatigue performance. The applied cyclic loading will cause compression force in the bar. The top bar starts at yield due to the jacking force. The application of the 0.5 kip minimum fatigue load will cause some compression thereby reducing the stress level below yield. Increasing to the maximum load will cause further compression in the top bar. The result is a tensile stress range in the bar where the maximum stress is below yield.
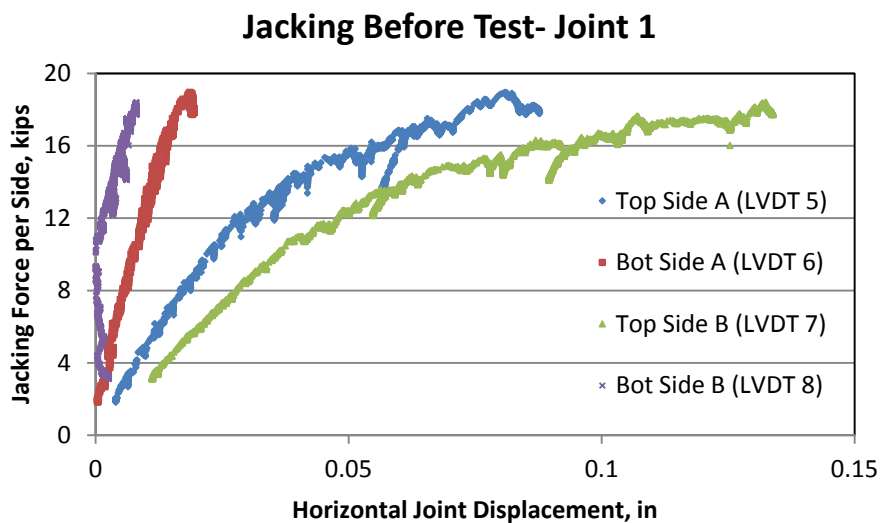
Jacking Before Test- Joint 1

Figure 30. LVDT Readings at Joint 1 During Jacking

The longitudinal joint opening deflection for both sides of Joint 1 is shown in Figures 31 and 32. The magnitude is significantly larger compared to the I-81 specimens without the jacking force. This increase can be explained by the absence of concrete contact and possible local debonding of the reinforcing bars at the edges of the joint. Similar to the unjacked specimens, there is a trend toward increased joint opening as cycles are accumulated on the specimen. This is likely due to additional changes in the local bonded length of the bars adjacent to the joint. There are notable differences between the opening response at the two sides of Joint

30

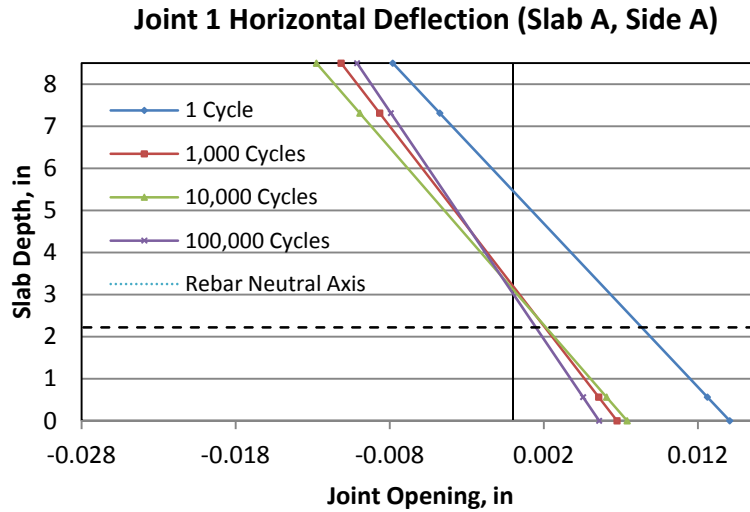1. The reason for this difference is not known but may relate to eccentricities of the reinforcing bar group.

Joint 1 Horizontal Deflection (Slab A, Side A)

Figure 31. Opening of Joint 1 (Specimen A, Side A)

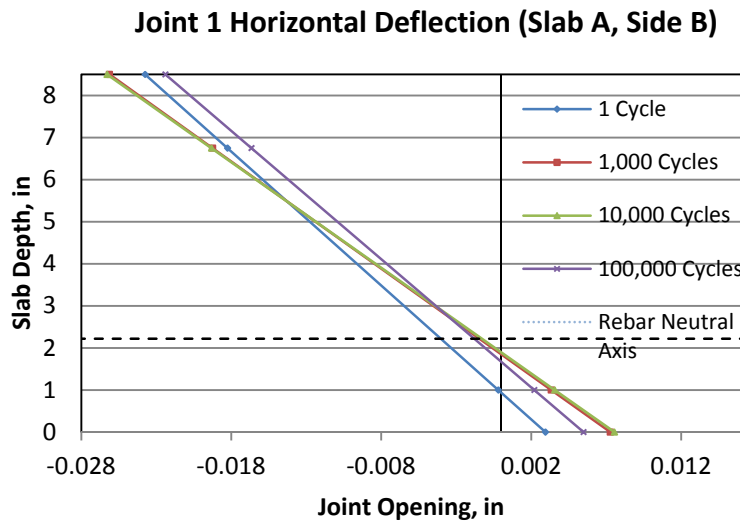**Joint 1 Horizontal Deflection (Slab A, Side B)**

Figure 32. Opening of Joint 1 (Specimen A, Side B)

In notable contrast to the I-81 specimens, Specimen B showed significant differential vertical deflection across the joints under cyclic loading. There were also significant differential vertical deflections across the joints for strength test Specimen A with the joints jacked open. This clearly shows the difference between joints with and without concrete contact. Figure 33 shows that the differential vertical deflection decreases after the first 1000 cycles of loading and remains relatively constant thereafter. This is possibly due to initial local crushing of the concrete around the reinforcing steel in the joint area.

Average Deflection Across Joints
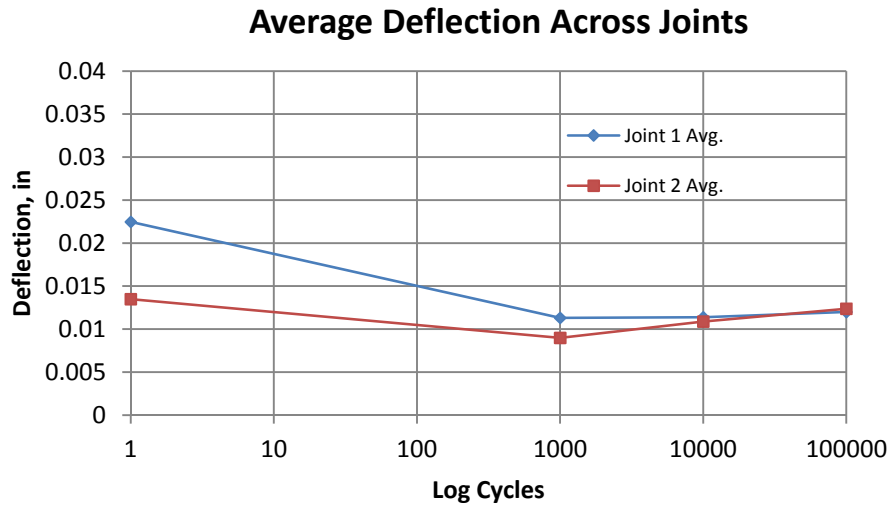
Figure 33. Change in Differential Vertical Joint Deflection As a Function of Fatigue Cycling

The top reinforcing bar in Specimen A failed in fatigue after 282,000 cycles under a cyclic load range of 16 kips. This contrasts with the I-81 specimens that showed no failure after 10 million cycles. The difference can be attributed to the presence of differential vertical displacement across the joints in Specimen A. Figure 34 shows the failed joint in the loading fixture after the jacking struts were removed. The break of the top bar allowed the joint to rotate open at the top. There is also an appreciable differential vertical deflection of the failed joint. In the actual bridge, the joint rotation would be restrained and only the differential vertical deflection would have been evident. Therefore the specimen failure is consistent with the observed failure in the bridge.

Figure 35 shows the fatigue failure surface of the top reinforcing bar after the joint was opened to expose the bar. Examination of the failure surface clearly shows that the fatigue crack initiated at the top of the bar and propagated downward until about 2/3 of the bar area was cracked. The bottom region shows a tension overload failure that occurred on the reduced net section. The small areas of corrosion occurred after the failure due to humidity in the air and did not participate in the failure. The failure surface is similar to those observed by Helgason et al. (1976) where the bars failed under flexural tension. While Helgason et al. reported that the failures initiated at the edge of a deformed rib on the bar, the failure in Specimen A appears to originate at an undeformed region of the bar. The top fatigue cracked region of the bar closely resembles the texture of the surface of the failed bars in the I-81 bridge. However the lower tension overload region was not observed in the I-81 bridge. This can be explained by the difference in rotational restraint between Specimen B and the continuous slab in the bridge. The rotational restraint would not allow enough joint opening displacement to cause tension failure in the bar. Instead, it is likely that the fatigue crack would continue to propagate through the entire cross section. The presence of multiple bars in the bridge provide load shedding paths that will delay fracture instability of the fatigue crack. Accounting for the differences caused by the

32

boundary conditions, it can be concluded that the failure surfaces of some of the bars in the I-81 bridge are consistent with the fatigue failure observed in Specimen A.

The differential vertical joint deflections (shear deformations across the joint) will add significant local stress in reinforcing bars spanning the joint. Figure 36 shows the three deformation mechanisms reported by Park and Paulay (1975). The fatigue crack initiated at the top of the bar about 0.67 in away from the plane of the joint. This location is consistent with the location of maximum stress caused by either the bending or kinking mechanism under the differential vertical displacement of the joint. Some localized concrete crushing must have occurred around the reinforcing bars to allow formation of either of these mechanisms.

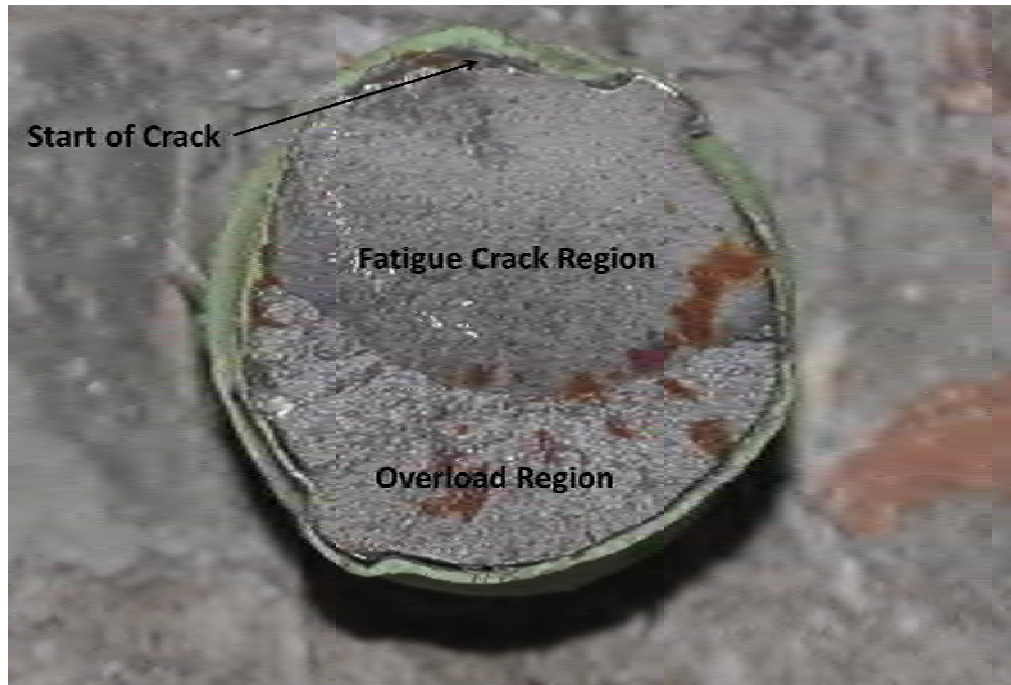**Figure 34. Joint Fatigue Failure in Specimen A**

Figure 35. Fatigue Failure Surface of Top Bar in Joint 1
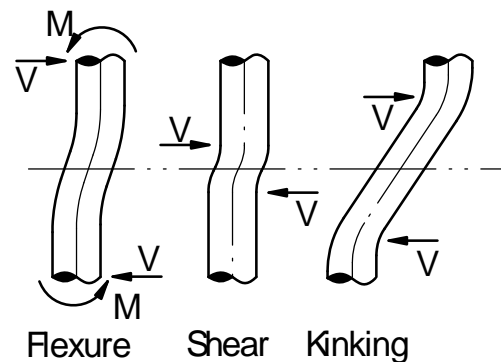

Flexure   Shear   Kinking

Figure 36. Three Force Transfer Mechanisms for Dowel Action across a Concrete Joint (after Park and Paulay, 1975)

Based on statistical analysis of their tests, Helgason et al. (1976) arrived at the following equations to predict fatigue life of reinforcing bars under axial load:

$$logN = 6.9690 - 0.0383f_r \qquad (2)$$

$$logN = 6.9690 \pm 0.3586 - 0.0383f_r \qquad (3)$$

Equation 2 represents the mean life and Equation 3 represents the upper and lower 95% statistical bounds on the data. Here N is the number of cycles at failure and f_r is the stress range. Substituting $N = 282,000$ cycles in Equation 3, the stress range in the reinforcing steel can be estimated to be between 30.3 and 49.0 ksi (39.7 ksi mean). It is difficult to calculate stress

34

ranges under the local bending mechanisms shown in Figure 36 without knowing the internal interaction with concrete crushing. However, it can generally be stated that 49 ksi stress range is possible given the differential vertical deflection observed in the test. Without the local bending effects, the stress range in the reinforcing steel can be expected to be below the fatigue threshold and infinite life would be expected.

Field Tests

A simple field test can be done to evaluate the fatigue susceptibility of cold joints that lack shear key engagement of the concrete across the joint. A simple dial indicator with 0.001 in resolution or better can be mounted to a steel plate and placed to measure differential vertical displacement between the two sides of the joint. A loaded truck can then be placed to put a loaded wheel on the closure pour joint. Depending on the joint location, multiple wheel load placements may be indicated. If there is no measurable differential deflection then fatigue failure is unlikely.

CONCLUSIONS

- *Fatigue of reinforcing steel is possible under conditions that introduce localized bending at closure pour joints.* Two specific conditions are required to allow localized bending: (1) the joint must be located away from beams or other means of vertical support; and (2) the joint must not have any concrete-to-concrete shear transfer across the joint. In this case, all shear and axial force across the joint is carried by the reinforcing steel alone, resulting in high stress ranges due to localized bending of the reinforcing steel.

- *Differential vertical deflection between the two sides of the joint is a necessary condition for fatigue to occur in deck joints.* The differential deflection induces local bending stress in the reinforcing steel that is additive to the stress range due to global bending. Localized bending will not be significant in joints where there is no measurable differential vertical deflection under wheel loads.

- *Insufficient data exist to relate fatigue resistance to the magnitude of differential joint deflection.* Lacking such data, any differential joint deflection (0.001 in or greater) under application of a wheel load should be considered an indicator that fatigue is possible. The absence of differential vertical deflection provides a high confidence that fatigue will not occur.

- *The failure mechanism observed in the strength tests does not match the observations of the I-81 deck failure.* The tests indicate some degree of punching shear would be expected if failure occurred under overload wheel loads. Even considering the section loss of some bars due to corrosion, the I-81 failures do not appear to be strength failures.

- *The failure plane of the reinforcing steel across the joint was vertical and the failed surfaces were relatively flat and smooth.* This is consistent with observations of bars failed by

fatigue. This fact, along with the unlikelihood of strength failure, makes fatigue the most probable cause of failure. Section loss due to corrosion can be expected to increase localized stresses in the bars and likely was an accelerator for fatigue damage.

- New deck joints should be designed to provide shear transfer between the concrete on either side of the joint. Alternatively, the joints should be located over beams or other means of vertical support. Shrinkage and constraint across the joint should also be minimized to reduce vulnerability to corrosion.

RECOMMENDATION

1. *VDOT's Structure and Bridge Division should always detail shear keys at cold joints. However, the construction of shear keys at the joint between the closure pour and the previously cast bridge deck studied in this project is not practical. Alternatively, joints should be located where there is structural support on each side.*

BENEFITS AND IMPLEMENTATION PROSPECTS

This study has revealed the susceptibility of smooth-faced construction joints between phases of deck construction to fatigue failure of the reinforcing steel under certain specific conditions. The conditions require no concrete-to-concrete shear transfer across the joint and constraint conditions that cause the joints to open when the concrete shrinks. The presence of these conditions can be easily detected by measuring the differential vertical displacement occurring across the joint under wheel loads. In the absence of vertical deflection, the reinforcing steel can be expected to have infinite fatigue life.

The inspection and maintenance recommendations are to inspect joints carefully for leaking and seal joints to prevent ingress of corrosion inducing substances. The implementation of these recommendations should prevent future failures of previously constructed decks with similar details.

ACKNOWLEDGMENTS

REFERENCES

Abbas, E.K., Weyers, R.E., Roberts-Wollmann, C.L., and Wright, W.J. *Corrosion Assessment for the Failed Bridge Deck Closure Pour at Mile Marker 43 on I-81.* VCTIR 14-R13. Virginia Center for Transportation Innovation and Research, Charlottesville, 2014.

Helgason, T., Hanson, J.M., Somes, N.F., Corley, W.G., and Hognestad, E. *Fatigue Strength of High-Yield Reinforcing Bars.* NCHRP Report 164. Transportation Research Board, Washington, DC, 1976.

Park, R., and Paulay, T. *Reinforced Concrete Structures.* John Wiley & Sons Inc., New York, 1975.

Sprinkel, M.M., Weyers, R., Blevins, C., Ramniceanu, A., and Weyers, S.A. Failure and Repair of Deck Closure Pour on Interstate 81. In *Transportation Research Record: Journal of the Transportation Research Board,* No. 2150(1), 2010, pp. 119-128.